RESEARCH ARTICLE   OPEN ACCESS

Robust Control Based On Sliding Mode of the Shunt Active Filter to Compensate For the Disturbing Currents in the Electric Power

Tarik Jarou[1], Nabil Elhaj[2] And Anass Ait Laachir [3]

[1]Associate Professor, Department of Electric Engineering, National School of Applied Sciences, Ibn Tofail University, Kenitra, MOROCCO.
[2]Student Searcher Laboratory for High Energy and Engineering Sciences, Ibn Tofail University, Kenitra, MOROCCO,
[3]Student Searcher Laboratory for High Energy and Engineering Sciences, Ibn Tofail University, Kenitra, MOROCCO.

ABSTRACT
The present publication articulates on the robust control strategy of the shunt active power filter (SAPF) originally based on the sliding mode. The new control strategy is tested to control the SAPF to compensate actively for the disturbing currents in the electric power under the presence of the voltage disturbances. The simulation results reveal a perfect compensation for the currents disturbances and the reactive power with a contribution to improve the robustness in stability and in speed of the SAPF. The efficiency of the proposed control strategy contribute to the improvement of the supply current spectrum and the phase displacement factor. Consequently, the control strategy proposed allows the SAPF to improve the energy quality.
Keywords- Shunt active power filter; Robust control; Sliding mode; Digital simulation; Energy quality

I. INTRODUCTION

Following the liberalization of the electrical energy and the generalization of the generator equipment of electric disturbances, the provider and the customer of electrical energy have to mobilize to assure the energy quality. The active filter can be envisaged to assure this quality.

This research action has for objective the improvement of the robustness in stability and in speed of the SAPF control strategy. The control strategy allows the SAPF to compensate for the big part of the currents disturbances generated by the various polluting load (Static converter, Driver Motor…)[2] [3].

The efficiency and the robustness of the studied strategy will be experienced in the SAPF control with the presence of the supply voltage disturbances (harmonics, imbalance in amplitude, off-peak and the frequency drift).

II. STUDIED SYSTEM

The studied system, as Figure 1 shows, consists of an tree-phase supply (Vs, Rs, Ls), an polluting load and a shunt active power filter [1] [2] [3] [4].

The polluting load consists of a unbalanced resistive load in shunt with a double three-phase rectifier based on thyristors. The rectifier is loaded by a passive circuit (rd, Ld) simulating a DC load [6][10]. Consequently, the polluting load are a no linear, unbalanced and absorbs the reactive power

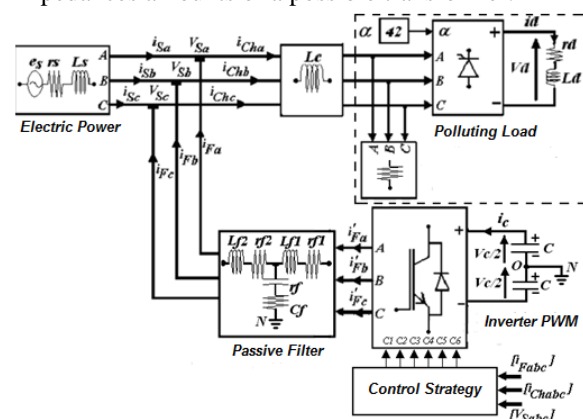[3]. The inductance (Lc, rc) represents the impedances amounts of a possible transformer.

Figure. 1 Block diagram of the electric system studied

The active filter is structured around a three phase inverter PWM constituted by three half-bridges (T1-T4, T2-T5 and T3-T6) based on the transistor IGBT with a diode in anti-shunt line [6] [10]. The inverter is supplying by a capacitive divisor with the neutral point N connected to the middle point O. Such a choice of this structure has for objective to separate the control of the tree half-bridge as well as to decouple the system and simplify the synthesis of the SAPF control law.

The passive filter at the input of the inverter allows reducing the harmonics caused by the PWM control. The voltage of the condenser C is supposed

regulated with a continuous regulation which is not treated in this study.

The switches states of T1, T2 and T3 are respectively complementary of those T4, T5, T6 and controlled by the following vector:

$$[C] = \begin{bmatrix} C_1 & C_2 & C_3 \end{bmatrix} \quad (1)$$

Where the signal Ci (1/0) represents the switching function of the switch Ti (closed/open) with i=1,2 or 3. We define three voltage of the inverter compared with the neutral point N by the vector of following voltage [10]:

$$[V_F] = \begin{bmatrix} V_{FA-N} & V_{FB-N} & V_{FC-N} \end{bmatrix} (2)$$

The expression which takes the vector [V$_F$] verifies the following equation [10]:

$$[V_F]^T = \frac{Vo}{2} \begin{bmatrix} 1 & 0 & 0 \\ 0 & 1 & 0 \\ 0 & 0 & 1 \end{bmatrix} \cdot [C]^T \quad (3)$$

According to the relation (3), we deduct that every inverter output depends only on a single control input Ci (i=1,2 or 3). Consequently, the control study of our three-phase system amounts to the single-phase system governed by the following differential equations:

$$\begin{cases} C_f \cdot \dfrac{dv_{Cf}}{dt} = i'_F - i_F \\[2mm] L_{f2} \cdot \dfrac{di_F}{dt} = v_{Cf} - v_S - r_{f2} \cdot i_F \\[2mm] L_{f1} \cdot \dfrac{di'_F}{dt} = v_F - v_{Cf} - r_{f1} \cdot i'_F \\[2mm] v_F = \dfrac{V_0}{2} \cdot C \end{cases} \quad (4)$$

III. PROPOSED CONTROL STRATEGY

The proposed control strategy for the SAPF, as mentioned in Figure. 2, consists of a [5]:
- calculation block of SAPF reference currents which allows to identify the disturbances current to compensate with the SAPF.
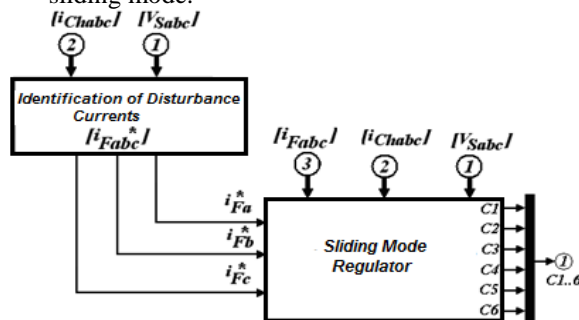- regulation block of SAPF current based on sliding mode.

Figure. 2 Block diagram of the control strategy proposed for the system

3.1 Robust calculation of the current references

In front of the frequency variation (50/60Hz±10%) and in the presence of the disturbances (harmonics, imbalance, off-peak ,….) affecting the supply voltage, the identification of the disturbances currents requires a parfait precision [5].

On the basis of our already published research works [1] [2], we synthesized a robust method to calculate exactly the currents references of the SAPF.

Theprinciple of the method consists in detecting the phase θs (t) of the voltage supply V$_S$ in real time. The phase synchronous detector, as Figure 3 shows, use a digital PLL to generate exactly the terms of synchronization(sinθ$_S$, cosθ$_S$).

Indeed, the signal received on the input of the detector, is shaped by a sign comparator and applied to a digital PLL which the phase comparator has a phase originally null . If the supply frequency stays in the capture rang of the PLL (45<Fs<65Hz), the oscillator VCO delivers a signal of frequency 256*Fs. Thereturn is realized through a counter which divides the signal frequency of the VCO by 256.

The output signal s(t) of the converter Digital/Analog has an asymmetric triangular shape which the frequency is regulated to the frequency input signal.
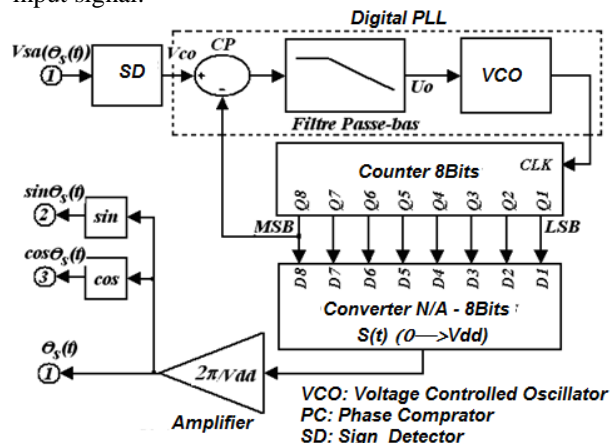
Figure 3. Schéma bloc du détecteur synchrone de la phase instantanée du signal VSa à base d'une PLL numérique

The calculate of SAF references currents consists to determine the disturbance currents [i$_{Chabc\_p}$] of currents load, by eliminating the direct systems of the fundamental frequency [i$_{Chabc\_f}$] to the load currents [i$_{Chabc}$].

In the design of this block, as Figure 4 shows, we envisaged two options of compensation to assure a flexible correction of the power reactive by a simple action on signal bit in the block control (1/0 →Compensation Yes/No).

The first option bases on the compensation of the disturbance currents [i$_{Chabc\_p}$] without compensating for the reactive power. In this case, we

improve the form factor of supply current, the power factor without touching the phase displacement factor cosφ. The reference currents of the SAPF are calculated by:

$$\left[i_{Fabc}*\right] = C_{32}^{-1} \begin{bmatrix} i_{Ch\alpha} - i_{Ch\alpha\_f} \\ i_{Ch\beta} - i_{Ch\beta\_f} \end{bmatrix} (5)$$

Where:

$$\begin{bmatrix} i_{Ch\alpha\_f} \\ i_{Ch\beta\_f} \end{bmatrix} = I_{Ch1} \cdot \sqrt{\frac{3}{2}} \begin{bmatrix} \sin\theta \\ -\cos\theta \end{bmatrix} (6)$$

The term I_{Ch1} represents the direct systems amplitude of the fundamental frequency which we calculate with the following relation:

$$I_{Ch1} = \sqrt{\frac{2}{3}} \cdot \sqrt{<i_{Ch\alpha}^2 + i_{Ch\beta}^2>} \quad (7)$$

The second option suggests compensating of the disturbance currents [i$_{Chabc\_p}$] and compensating for the reactive power. In this case, we develop positively, at the same time, the form factor μi and the THDi of the supply current, the power factor λi and the phase displacement factor cosφ. The reference currents of the SAPF are calculated by the following relation:

$$\left[i_{Fabc}*\right] = C_{32}^{-1} \begin{bmatrix} i_{Ch\alpha} - i_{Ch\alpha\_fa} \\ i_{Ch\beta} - i_{Ch\beta\_fa} \end{bmatrix} (8)$$

Where:

$$\begin{bmatrix} i_{Ch\alpha\_fa} \\ i_{Ch\beta\_fa} \end{bmatrix} = I_{Ch1a} \sqrt{\frac{3}{2}} \begin{bmatrix} \sin\theta_S \\ -\cos\theta_S \end{bmatrix} (9)$$

The term I_{Ch1a} represents the active component to the fundamental frequency of the disturbance currents [i$_{Chabc\_p}$] which we calculate with the following relation:

$$I_{Ch1a} = \sqrt{2/3} <i_{Ch\alpha} \cdot \sin\theta_S - i_{Ch\beta} \cdot \cos\theta_S> (10)$$
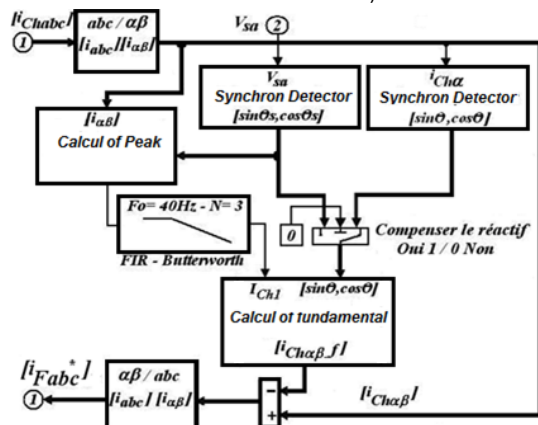

Figure 4. Block diagram of the strategy suggested to calculate the SAPF references

3.2 Robust control strategy based on sliding mode
3.2.1 State model of the system

The studied system is a not linear systems witch the not linearity is introduced by the voltage control Ci (i=1,2 or 3). The mathematical model of the system is governed by the differential equations of the relation (4) which describe the behavior of the single-phase system [7][8].

We note the various electric terms of the system as follows:

$$\begin{cases} x_1 = i_F', x_2 = v_{Cf}, x_3 = i_F \\ \quad u = C, p = v_S, y = i_F \ (11) \\ \varsigma_f = 1/C_f, \ell_1 = 1/L_{f1}, \ell_2 = 1/L_{f2} \\ \tau_1 = r_{f1}/L_{f1}, \tau_2 = r_{f2}/L_{f2} \end{cases}$$

Where the electric quantity u, p, and X(x$_1$,x$_2$,x$_3$) are respectively, as shown in Figure 4., the voltage control, the disturbance, the input of the system and the components of the state vector. Considering the following state vector:

$$X^T = \begin{pmatrix} x_1 & x_2 & x_3 \end{pmatrix} (12)$$

The state model of the system, according to the relation (4), (11), (12) and (13), can be expressed as:

$$\begin{cases} \dot{X} = A.X + B.u + B_p.p \\ y = C^T.X \end{cases} (13)$$

Where :

$$\begin{cases} A = \begin{bmatrix} -\tau_1 & -\ell_1 & 0 \\ \varsigma_f & 0 & -\varsigma_f \\ 0 & \ell_2 & -\tau_2 \end{bmatrix} \\ B^T = \frac{V_0}{2}\ell_1.\begin{pmatrix} 1 & 0 & 0 \end{pmatrix} \\ B_P = \begin{pmatrix} 0 & 0 & -\ell_2 \end{pmatrix} \\ C^T = \begin{pmatrix} 0 & 0 & 1 \end{pmatrix} \end{cases} (14)$$

Finally, we conclude that the system have state model of tree order, no linear, invariant and disturbed [7]. The non-linearity is introduced by the control voltage u. This model proposed of the electric system, is able reporting efficiency the system dynamics with the aim to control and simulate the studied system.

3.2.2 State model of the system in the sliding mode

The regulation in sliding mode is realized by rely control u (1/-1) [5]. The regulation system has a variable structure with feedback state [8].

The three-phase inverter based on transistors IGBT and controlled by a electric term u which is imposed by a control law governed by the following relation:

$$S(X) = -K^T.X + k_C.y_C \quad (15)$$

Where K is the vector line gain of feedback state and S(X) is the switching plan of sliding mode governed by:

$$S(X) > 0 \Rightarrow u = +1$$
$$S(X) < 0 \Rightarrow u = -1 \quad (16)$$

For the system dynamic in sliding mode, the state vector follows a trajectory which respects the following condition:

$$-\Delta S \leq S(X) \leq +\Delta S \quad (17)$$

By consideration of the switching plan in this rang ($|\Delta S| < \pm\Delta S$, $\Delta S = 0.1$) allows the law control to limits the switching frequency of the inverter. Afterward, we shall suppose ΔS infinitesimal to facilitate the control law synthesis.

The switching plan with a regulator based on sliding mode is given onto Figure 5. Considering the following notations:

- y_C is the reference of system i_{Fi}* avec i=a, b or c,
- y is the output of system i_{Fi} avec i=a, b or c,
- u is the control voltage Ci avec i=1, 2 or 3
- K is the gain vector lines of the feedback state,
- K_C is the coefficient of the direct intervention of the reference,

We obtain the state model in sliding mode of the global system [8] as follows:

$$\begin{cases} \dot{X} = A_g X + B_{pg} p + B_{Cg} y_C + B'_{Cg} \dot{y}_C \\ y = C^T.X \end{cases} \quad (18)$$

The matrices of this state model become in sliding mode:

$$\begin{cases} A_g = (1 - \dfrac{1}{K^T B} B.K^T).A \\[2mm] B_{Pg} = (1 - \dfrac{1}{K^T B} B.K^T).B_P \\[2mm] B_{Cg} = (1 - \dfrac{1}{K^T B} B.K^T).B_C \\[2mm] B'_{Cg} = \dfrac{k_C}{K^T B}.B \end{cases} \quad (19)$$

3.2.3 Synthesis of the control law

The synthesis of the control law consists in determining the coefficients of the gain state vector K. By making a basic change in the canonical space of controllability by a lineartransformation with a matrix T that we suppose constant, square and regular [7] [8], the new state vector is given by:

$$\overline{X} = T.X \quad (20)$$

The linear transformation matrix T is defined as:

$$T^T = \begin{pmatrix} t^T & t^T A & t^T A^2 \end{pmatrix} \quad (21)$$
$$t^T Q_C = \begin{pmatrix} 0 & 0 & 1 \end{pmatrix}$$

Where Q_C is the controllability matrix in the initial space and also be expressed as:

$$\begin{cases} Q_C = \begin{pmatrix} B & AB & A^2 B \end{pmatrix} \\[2mm] Q_C = \dfrac{V_0 \ell_1}{2} \begin{pmatrix} 1 & -\tau_1 & \tau_1^2 - \ell_2 \varsigma_f \\ 0 & \varsigma_f & -\tau_1 \varsigma_f \\ 0 & 0 & \ell_2 \varsigma_f \end{pmatrix} \end{cases} \quad (22)$$

The system model regulated by the sliding mode becomes in the canonical space of controllability:

$$\begin{cases} \dot{\overline{X}} = \overline{A}_g \overline{X} + \overline{B}_{pg} p + \overline{B}_{Cg} y_C + \overline{B}'_{Cg} \dot{y}_C \\ y = \overline{C}^T \overline{X} \end{cases} \quad (23)$$

Where :

$$\overline{A}_g = \begin{bmatrix} 0 & 1 & 0 \\ 0 & 0 & 1 \\ -\alpha_0 & -\alpha_1 & -\alpha_2 \end{bmatrix} \quad (24)$$

They terms α_i represent the coefficients of characteristic equation $\Delta'(s)$ of the system regulated in the canonical space of controllability [7].

Because the matrix Q_C is regular (rank(Q_C)=3) then the system is controllable and we can calculate the feedback state in the canonical space of controllability and to assignarbitrarily they poles to the regulated system. Afterward the matrix T is calculated using:

$$\begin{cases} t^T = \dfrac{2}{V_0 \ell_1} \begin{pmatrix} 0 & 0 & 1/\ell_2 \varsigma_f \end{pmatrix} \\[2mm] T = \dfrac{2}{V_0 \ell_1} \begin{bmatrix} 0 & 0 & 1/\ell_2 \varsigma_f \\ 0 & 1/\varsigma_f & -\tau_2/\ell_2 \varsigma_f \\ 1 & -\tau_2/\varsigma_f & (\tau_2^2/\ell_2 \varsigma_f) - 1 \end{bmatrix} \end{cases} \quad (25)$$

In the initial space, the feedback state vector $K^T = \begin{pmatrix} k_1 & k_2 & k_3 \end{pmatrix}$ is calculated by [7]:

$$K^T = \begin{pmatrix} \alpha_1 & \alpha_2 & 1 \end{pmatrix} T \quad (26)$$

The coefficients α_i are linked to the poles assigned (s_0, s_1, s_2) to the regulated global system which the characteristic equation $\Delta'(s)$ is defined as[7]:

$$\Delta'(s) = |s.1 - \overline{A}_g| = (s - s_0).(s - s_1).(s - s_2) \quad (27)$$

The matrix $\overline{A}_g$ is singular and the pole s0 must be equal to zero ($s_0 = 0$) and the other poles can be arbitrarily chosen [7] [8]. On the other hand, the poles s1 and s2 must be conjugated and possess a negative real part to insure a stable behavior in

sliding mode and have an optimal relative amortization($\zeta=0.707$).

So, if we impose for the regulated system the following poles:

$$s_0 = 0, s_{1,2} = -\rho \pm j\rho \quad (28)$$

The transfer function of the regulated system is giving by:

$$F_{BF}(s) = \frac{V_0 \ell_1 \ell_2 \varsigma_f}{2} \frac{1}{2\rho^2 + 2\rho.s + s^2} \quad (29)$$

In steady state, the regulated system reference y_C is different from the regulated system output y. Then the coefficient k_C of the reference is used to cancel the static error and reckoned by:

$$k_C = 1/F_{BF}(0) = \frac{4\rho^2}{V_0 \ell_1 \ell_2 \varsigma_f} \quad (30)$$

The absolute value of the real part of s_1 and s_2 will be adjusted to realize a good compromise between the regulation speed and the sliding domain [8].
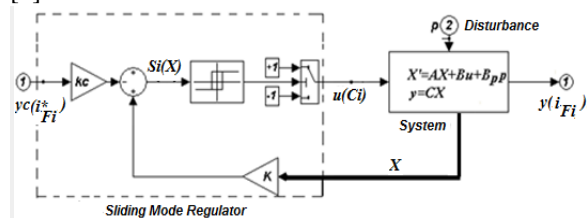

Figure 5. Block diagram of the control law based on sliding mode

IV.   RESULTS OF SIMULATION

The digital simulation is given in the environment Matlab/Simulink - Power System Blockset. The simulated system is given onto the previous figures (See Figure 1, 2, 3, 4, 5) with parameters listed in Table 2 and Table 3.

The digital simulation results show that the SAPF control based on sliding mode compensates perfectly for the disturbing currents and the reactive power, with a stable and fast dynamics in the following cases:
-   supplying of a no linear and unbalanced polluting load which absorb the reactive power as shown in Figure 6-c, 8-c, 10-c, 12-cand 14-c (Evolution of DC load: $\alpha=42° \rightarrow 10°$ at t=0.05s).
-   supplying a polluting load with a voltage supply strongly disturbed : Voltage supply affected with harmonics (THDu =20 %), a two-phase of-peak($\Delta U/U_N$ =35%) and an unbalanced amplitude ($\Delta U_i =20\%$), as shown in Figure 6-a, 8-a, 10-a, 12-a and 14-a.

The temporal analysis results of the control by sliding mode, also show a perfect compensation for the current disturbances with contribution of the robustness in the SAPF dynamic performances. Indeed, we notice:

-   the extremely fast, precise and stable dynamic response to generate the currents of SAPF (Response Time <2ms, Relative Overflow < 1 %, etc.), as shown in Figure 6-d, 8-d, 10-d, 12-d, 14-d.
-   the trajectories of the state vector follow the switching plan in sliding mode in spite of the influence of disturbance and the reference variation as shown in Figure 7-a, 9-a, 11-a, 13-a.
-   he precision and the speed of the robust control is strong towards the evolution of the polluting load and the voltage supply strongly disturbed in as shown in Figure 6-d, 8-d, 10-d, 13-d.
-   the sliding mode persists without being interrupted by the disturbances supply, the system parameter variation and the reference variationas shown in Figure 7, 9, 11, 13.

We also recognize the good amortization of the transitory regime by a correct assignment made by the imposition method of the poles(p1,2= $\rho\pm$jρ).

The temporal and spectral analysis result, as shown in Figure 14 and 15, and recapitulated in the Table 1 and Table 4, prove the SAPF control strategy efficiency to reduce the total harmonic distortion of currents supply THDi, the degree of imbalance ΔIi and the form factor of the currents supply. As well as we note a clear improvement of the power factor λand of the phase displacement factor$cos\varphi$.
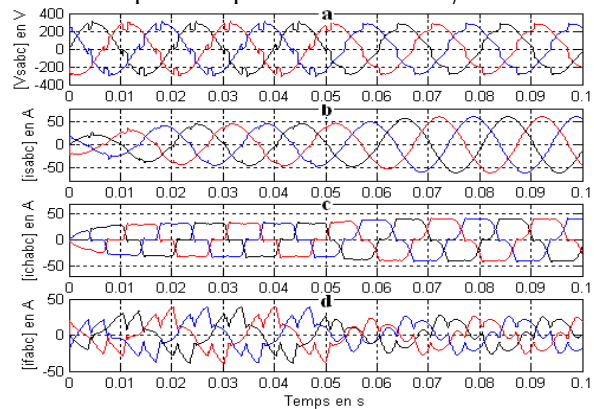

Figure 6.Temporal analysis of the sliding mode control of the SAPF under an load evolution at t=0.05s (Supply frequency 50Hz) a) Voltage supply b) Current supply c) Currents of the polluting load d) Currents compensation of the SAPF
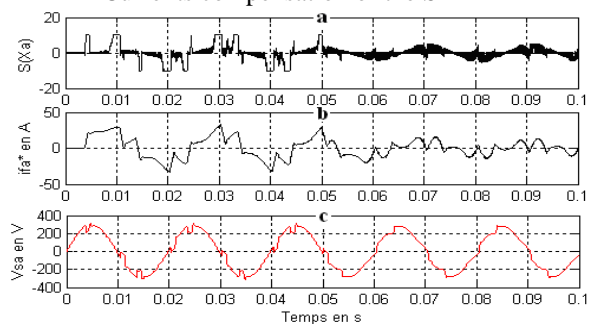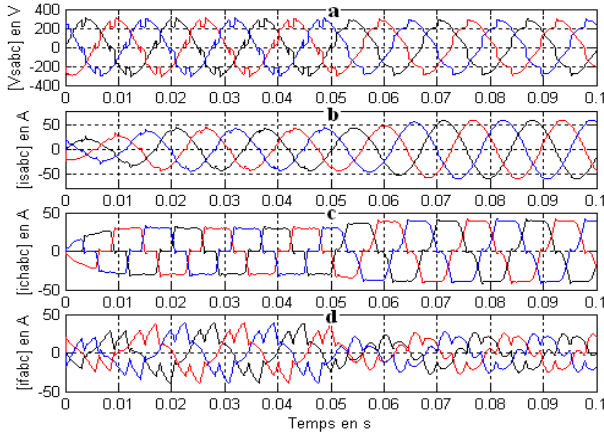
Figure 7.Temporal analysis of the sliding mode control of the SAPF under an load evolution at t=0.05s (Supply frequency 50Hz) a) Switching plan in sliding modeSa(Xa) under variation of i_F^* and V_S **b)** the reference of the control i_{Fa}^* **c)** the disturbance of the system V_{Sa}.

Figure 8.Temporal analysis of the sliding mode control of the SAPF under an evolution supply at t=0.05s (Supply frequency 60Hz) a) Voltage supply b) Current supply c) Currents of the polluting load d) Currents compensation of the SAPF
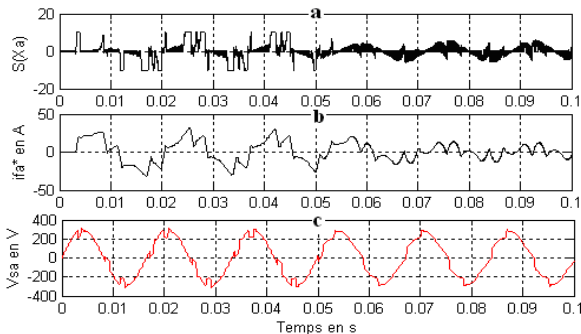

Figure 9.Temporal analysis of the sliding mode control of the SAPF under an evolution supply at t=0.05s (Supply frequency 60Hz) a) Switching plan in sliding modeSa(Xa) under variation of i_F^* and V_S b) the reference of the control i_{Fa}^* c) the disturbance of the system V_{Sa}.
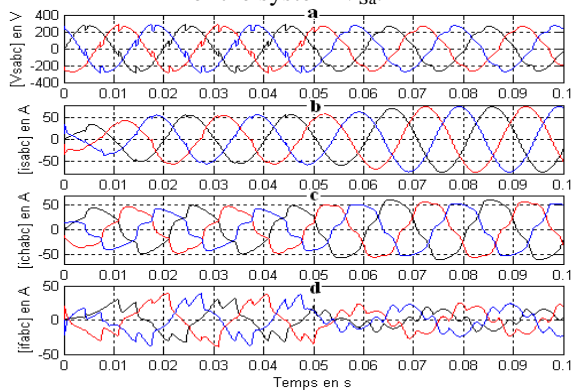

Figure 10.Temporal analysis of the sliding mode control of the SAPF under an unbalanced load and

load evolution at t=0.05s (Supply frequency 50Hz) a) Voltage supply b) Current supply c) Currents of the polluting load d) Currents compensation of the SAPF
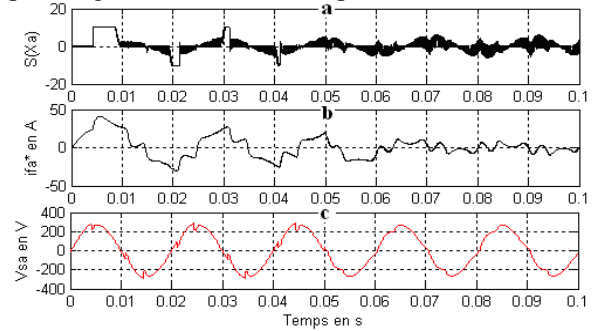

Figure 11.Temporal analysis of the sliding mode control of the SAPF under an unbalanced load and load evolution at t=0.05s (Supply frequency 50Hz) a) Switching plan in sliding modeSa(Xa) under variation of i_F^* and V_S **b)** the reference of the control i_{Fa}^* **c)** the disturbance of the system V_{Sa}
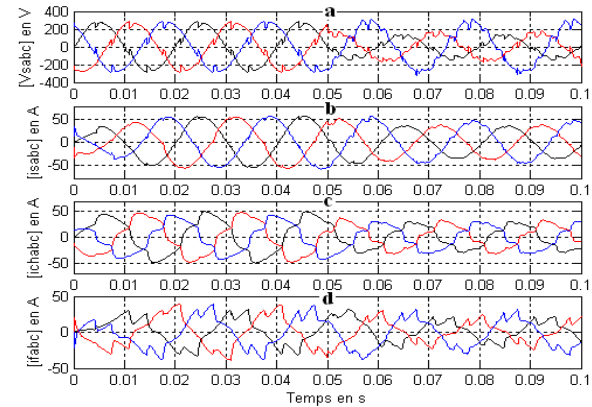

Figure 12.Temporal analysis of the sliding mode control of the SAPF under an unbalanced load and a supply affected by two phase off-peak (ΔU/UN =35%) and harmonics (THDu=20%) at t=0.05s (Supply frequency 50Hz) a) Voltage supply b) Current supply c) Currents of the polluting load d) Currents compensation of the SAPF
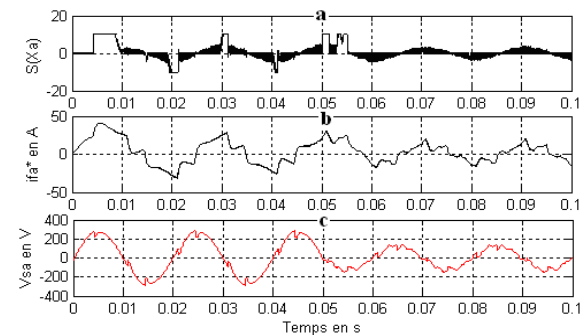

Figure 13.Temporal analysis of the sliding mode control of the SAPF under an unbalanced load and a supply affected by two phase off-peak (ΔU/UN =35%) and harmonics (THDu=20%) at t=0.05s (Supply frequency 50Hz) a) Switching plan in sliding

mode Sa(Xa) under variation of i_F* and VS b) the reference of the control $i_{Fa}*$ c) the disturbance of the system V_{Sa}
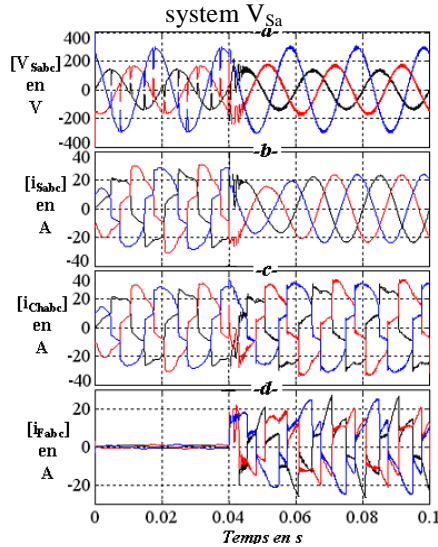

Figure 14.Temporal Analysis of the sliding mode control after insertion of the SAPF ar t=0.04s under an unbalanced load and a supply voltage affected by two phase off-peak (ΔU/UN =35%) and unbalanced amplitude (ΔUi =20%) at t=0.05s (Supply frequency 50Hz) a) Voltage supply b) Current supply c) Currents of the polluting load d) Currents compensation of the SAPF

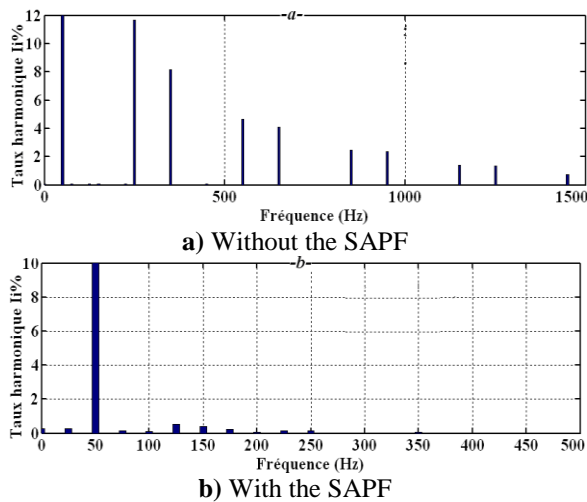**a)** Without the SAPF

b) With the SAPF

Figure 15. Spectral analysisof the supply currents

Disturbances characteristics	Without SAPF	With SAPF
Total harmonic distortion of currents of currents *THDi*	15.77%	0.16%
Form factor of currents μ_i	96.54%	99.97%
Displacement factor $cos\varphi$	0.90	0.98
Power factor λ	86.66	99.70

TABLE 1. Result of robust control strategy

V.   CONCLUSION

The first results of this research action allowed the digital validation under Matlab/Simulink environment of the robust control strategy originally based on the sliding mode to improve the performance of the shunt active power filter. The originality of this strategy consists in its robustness towards one a several disturbances of voltage supply and the system variation parameters.

Indeed, the digital simulation results, reveal a perfect compensation for the currents disturbance and a robustness in stability and in speed of the SAPF in front of a voltage supply strongly disturbed and an evolution of the polluting load.

The temporal and spectral analysis results prove the efficiency of the control strategy applied to the SAPF by allowing to compensate globally for the reactive power and for all the disturbances current generated by the polluting load. In brief, we notice a considerableimprovement of the supply currents spectrum and the power factor. Consequently, this research action contributes to generalize the shunt active power filters to improve the energy quality.

APPENDIX

Grandeur	*Description*
[V_{Sabc}]	Voltages supply vector
[i_{Sabc}]	Currents supply vector
[i_{Chabc}]	Currents load vector
[i_{Fabc}]	Currents load vector of SAPF
$cos\varphi$	Deplacement factor
$\theta(t) = \omega_S t - \varphi$	The instantaneous phase of fundamental of i_{Cha}.
α	Control angle of thyristor

TABLE 2. Nomenclature

Components of the system	Values of parameters
Supply voltages	e_S=220 V, f_S=50/60 Hz
Supply impedance	r_S= 500 mΩ - L_S=0.5 mH
Supply DC of inverter	V_{CO} = 740 V- C_O = 8.8 mF
Output filter of SAPF	L_{f1}=300μH - r_{F1} =1Ω L_{f2}=300μH - r_{F2} =1Ω C_f=150 μF - r_{f2}=0.5Ω

TABLE 3. Parameters of simulated system

Characteristics parameters of electric disturbances	
$\Delta U/U_N = U - U_N / U_N$	The off-peak depth of the voltage with U_N nominal effective value.
$\Delta Y_i = \lvert Y_{1\,i} \rvert // \lvert Y_{1d} \rvert$	the unbalance degree of current or voltage. Y_{1d} et Y_{1i} : Effective value of the positive and negative sequence of the fundamental one.
Y_1, Y_n	the effective value of fundamental and the harmonic of row n (of current or voltage)
$H_n \%$	Individual rate of harmonics. $H_n = 100.\ Y_n/\ Y_1$
$THD_y = 100.\sqrt{\sum\limits_{n=2}^{\infty} Y_n^2 / Y_1}$	The Total Harmonic Distortion.
$\lambda = \cos\varphi\,.\,\mu$	The Power Factor
$\mu = Y_1 / \sqrt{\sum\limits_{n=1}^{\infty} Y_n}$	The Form Factor
$\cos\varphi$	The Phase Displacement Factor

TABLE 4. Electrics characteristics of disturbances

REFERENCES

[1] T. Jarou, M. Cherkaoui, M. Maaroufi, Contributiontothecontrolingoftheshuntactive power filtertocompensatefortheharmonics, unbalancedcurrentsandreactive power *Proc. ofthe 6th WSEAS/IASME Int. Conf. on Electric Power Systems, High Voltages, Electric Machines*, Tenerife, Spain, December 16-18, 2006.

[2] T. Jarou, M. Cherkaoui, M.Maaroufi, Generalizationofthe Control StrategyoftheActive Filters toCompensatefortheDisturbingCurrentsandth eDisturbingVoltages, *WSEAS TRANSACTIONS on POWER SYSTEMS*, Issue 10, Volume 1, P1770-1776, ISSN 1790-5060, October 2006.

[3] F. Zheng Peng, ApplicationissuesofActive Power Filters, *IEEE IndustryApplications*, Vol. 4, N°5, Septembre / octobre, 1998.

[4] T.Thomas, K.Haddad, G.Joós et A.Jaafari, Design andperformanceofactive power filters, *IEEE IndustryApplications*, Vol. 4, N°5, Septembre/octobre, 1998.

[5] M.Machmoum, N.Bruyant, S.Saadate, M.Alali, Commandegénéralisée et analyse de performancesd'uncompensateuractifparallèle , *Revue Internationale de GénieÉlectrique*, VOL 4/3-4, 2001.

[6] M.A.E. Alali, *Contribution à l'étude des compensateursactifs des réseauxbassetension,* Thèse de doctorat en co-tutelle ULP Strasbourg et UHP Nancy ,septembre 2002.

[7] Chi-Tsong Chen, *Linear systemtheoryand design*, Edition Series Editor, ISBN 0-03060289-0 HRW, 1984

[8] HansruediBüuhler, *Réglage par mode de glissement*, Edition Presses polytechniquesromandes, ISBN 2-88074-108-4, 1986.

[9] G.GRELLET et G.CLERC, *Actionneursélectriques – PrincipesModèlesCommand*e, Editions Eyrolles, ISSN 2-212-09352-7, 1997.

[10] F. Labrique, G. Seguier et R.Bausiere, *la ConversionContinue-Alternative*, Documentation Lavoisier, pp. 73-88, 1995.

BIBLOGRAPHY

Tarik JAROU was born in Rabat, on 24th April 1973. He is University professor at the National School of the Sciences Applied of the University Ibn Tofail, Kenitra, Morocco. He received Doctoratdregree in Electric Engineering from the Engineer School Mohammedia of the University Mohamed V, Rabat, Morocco.

He is member of the research laboratory LHESIR of the University Ibn Tofail. His main area of research include the modelling and the control for electric systems control, the supervision of electric power sources with energy renewable and the implementation of the algorithms on the embedded systems.

NabilELHAJ was born in Tiflet, Morocco, on 7th November 1985. He received Master degree in Microelectronics from IBN TOFAIL University Kenitra, in July 2011. He is currently pursuing Ph.D degree in Electrical Engineering at laboratory LHESIR of IBN TOFAIL University, Kenitra, Morocco. His main area of research includes quality of electrical energy, Active Power filters and the electric power sources based on energy renewable.

Anass AITLAACHIRwas borninBeniMellal, Morocco, on 2th June 1988. He received Master degreein Microelectronics from IBN TOFAIL University Kenitra, in July 2011. He is currently pursuing Ph.D degree in Electrical Engineering at laboratory LHESIR of IBN TOFAIL University Kenitra, Morocco. His main area of research includes quality of electrical energy, Active Power filters and the electric power sources based on energy renewable